Alejandro Campos is a senior at the University of Rochester majoring in Mechanical Engineering and minoring in Physics. The research presented here was conducted at the Princeton Plasma Physics Laboratory in the summer of 2008 in the SULI program. In the summer of 2007, Alejandro conducted research at Caltech on an Output Mode Cleaner Suspension for the Laser Interferometer Gravitational-Wave Observatory. Alejandro was born in Lima, Peru, but considers San Francisco his hometown. He hopes to enter into a Ph.D. program in Aerospace Engineering with a concentration in Fluid Mechanics. Alejandro enjoys running in his free time.

Charles H. Skinner is a principal research physicist at the Princeton Plasma Physics Laboratory. He received his Ph.D. from the University of London for the first application of dye lasers to plasma diagnostics. He worked on the application of lasers to atomic physics at Harvard University and University of Colorado. After a brief period at the Physikalish-Technische Bundesanstalt in Berlin, Germany, he joined the Princeton Plasma Physics Laboratory and was part of a team that pioneered the first soft X-ray lasers. He has continued to work on magnetic fusion, in particular tritium retention and dust issues.

Advances in Dust Detection and Removal for Tokamaks

Alejandro Campos and Charles H. Skinner

ABSTRACT

Dust diagnostics and removal techniques are vital for the safe operation of next step fusion devices such as ITER. In the tokamak environment, large particles or fibers can fall on the electrostatic detector potentially causing a permanent short. An electrostatic dust detector developed in the laboratory is being applied to the National Spherical Torus Experiment (NSTX). We report on the development of a gas puff system that uses helium to clear such particles from the detector. Experiments at atmospheric pressure with varying nozzle designs, backing pressures, puff durations and exit flow orientations have given an optimal configuration that effectively removes particles from a 25 cm² area. Similar removal efficiencies were observed under a vacuum base pressure of 1 mTorr. Dust removal from next step tokamaks will be required to meet regulatory dust limits. A tri-polar grid of fine interdigitated traces has been designed that generates an electrostatic traveling wave for conveying dust particles to a "drain." First trials with only two working electrodes have shown particle motion in optical microscope images.

Introduction

Nuclear fusion is a promising alternative source of energy facing scientific and technical challenges. One of these challenges is the detection and removal of dust inside fusion reactors. Dust production results from the disassembly of plasma-facing tile surfaces or of co-deposited layers under intense transient heating by edge localized modes (ELMs) or disruptions. Dust can also appear as a result of the chemical agglomeration of sputtered C_n clusters [1]. Next step fusion devices, such as ITER, will produce larger quantities of dust, which could be radioactive from tritium or activated metals, toxic, and/or chemically reactive with steam or air [1]. The dust safety assessment value for ITER, which is the value above which the reactor's operation is unsafe, is 1 000 kg. However, due to accounting uncertainties, the largest quantity of dust allowed in the reactor, also known as the dust administrative limit, is 670 kg. The amount of hot dust inside a reactor has lower limits. The limits for hot dust are 6 kg each for beryllium, carbon and tungsten. However, when there is no carbon dust inside the reactor, the limits are 11 kg for beryllium and 77 kg for tungsten [2]. Dust detection and removal techniques, which are still in their infancy, are vital to the safe operation of fusion reactors.

An electrostatic dust detector has already been developed and tested [3]. This detector consists of a grid of interlocking circuit traces, which are biased to voltages ranging from 30 V to 50 V. Figure 1 shows a schematic of this device. A dust particle that falls on the detector causes a temporary short circuit, creating a voltage pulse recorded by standard nuclear counting electronics. The number of pulses is proportionally related to the mass of incident dust on the detector. The dust particles on the surface of the grid are usually vaporized or ejected from the detector, which restores the open circuit. However, some large particles or fibers stay on the surface and cause a permanent short circuit, which prevents the creation of further voltage pulses and impedes dust detection.

We have developed a gas puff system that blows helium gas on the surface of the detector to remove dust particles or fibers. A schematic of the gas puff system is shown in Figure 2. The system consists of a helium tank, a regulator, a shut-off valve that prevents or allows the flow of helium, a pressure meter that measures the gas pressure, a piezoelectric valve that controls the gas flow, and a nozzle through which helium is expelled. The piezoelectric valve is opened by a voltage pulse created by a pulse generator. This voltage pulse is monitored by an oscilloscope and is amplified by a driver. Gas is puffed in an inclined manner — the nozzle exit channel's longitudinal axis makes a 45° angle with the surface of the detector. This channel's diameter is 0.34 mm. The volume between the shut off valve and nozzle is 40.8 cm^3 and the volume between the shut off valve and piezoelectric valve is 31.0 cm^3. Our objective was to find the optimal gas puff system configuration that maximized the area of dust removed from the surface of the detector.

While the gas puff system clears dust from the surface of the electrostatic dust detector; the particles that are puffed away and other dust particles are deposited randomly on other areas inside the fusion reactor. Hence, another system is required to remove dust from the reactor itself. For this purpose, an innovative electrostatic dust transporter system that was recently designed and fabricated was tested.

Figure 3 shows a schematic of the electrostatic dust transporter system. The power supply generates three voltages, namely +V/2, ground and –V/2, which are transmitted to a triple rotary switch. This component sequentially switches the three voltages between the three electrodes of a tri-polar grid. The grid's electrodes branch out into fine interdigitated traces as shown in Figure 3. The resulting potential gradient on the surface of the tri-polar grid travels in a certain direction as the triple rotary switch sequentially switches the voltages. The potential gradient is repeated every three traces, resulting in a traveling electrostatic wave. A schematic of this wave is shown in Figure 4. Our objective was to test this system to observe particle motion and check the system's viability for dust removal. A more ambitious goal was to achieve consistent particle motion in one direction.

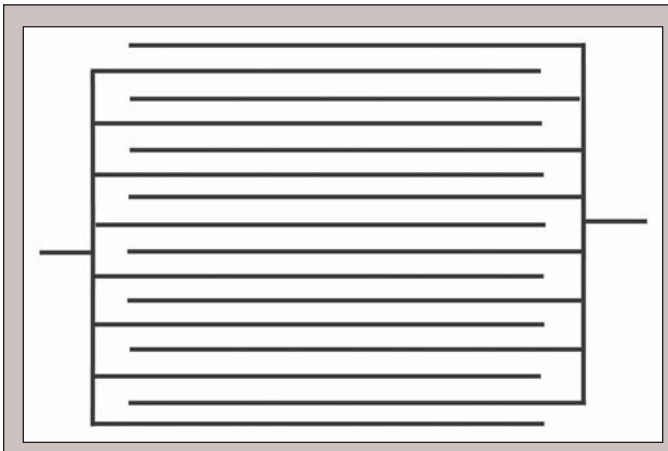

Figure 1. Schematic of the electrostatic dust detector is not drawn to scale. Particles falling in between the traces cause a temporary short circuit, which creates a voltage pulse that is recorded and related to the mass of incident dust.

Materials and Methods

Gas Puff System

A variety of short experiments was performed with the gas puff system to first investigate its properties and functioning. The highest voltage produced by the driver (corresponding to 20 half turns of the driver's control knob) best opened the piezoelectric valve. Nevertheless, this voltage was unknown since it was higher than the maximum value detected by the only available oscilloscope. The purpose of our first experiment was to predict the value of this high voltage. We measured different driver's output voltages detectable

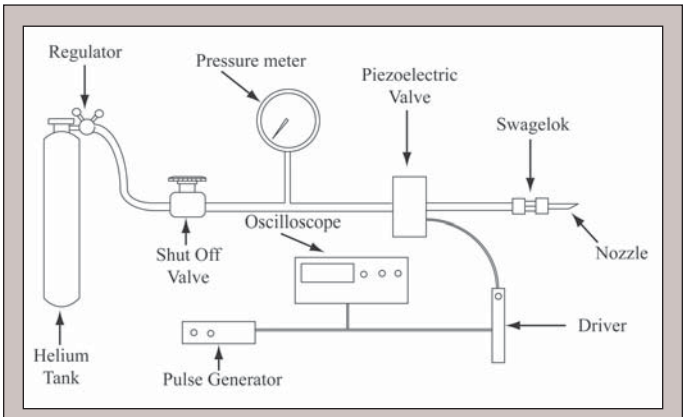

Figure 2. Schematic of the gas puff system, not to scale. Helium gas was blown through the system and was expelled at a 45° angle through the nozzle.

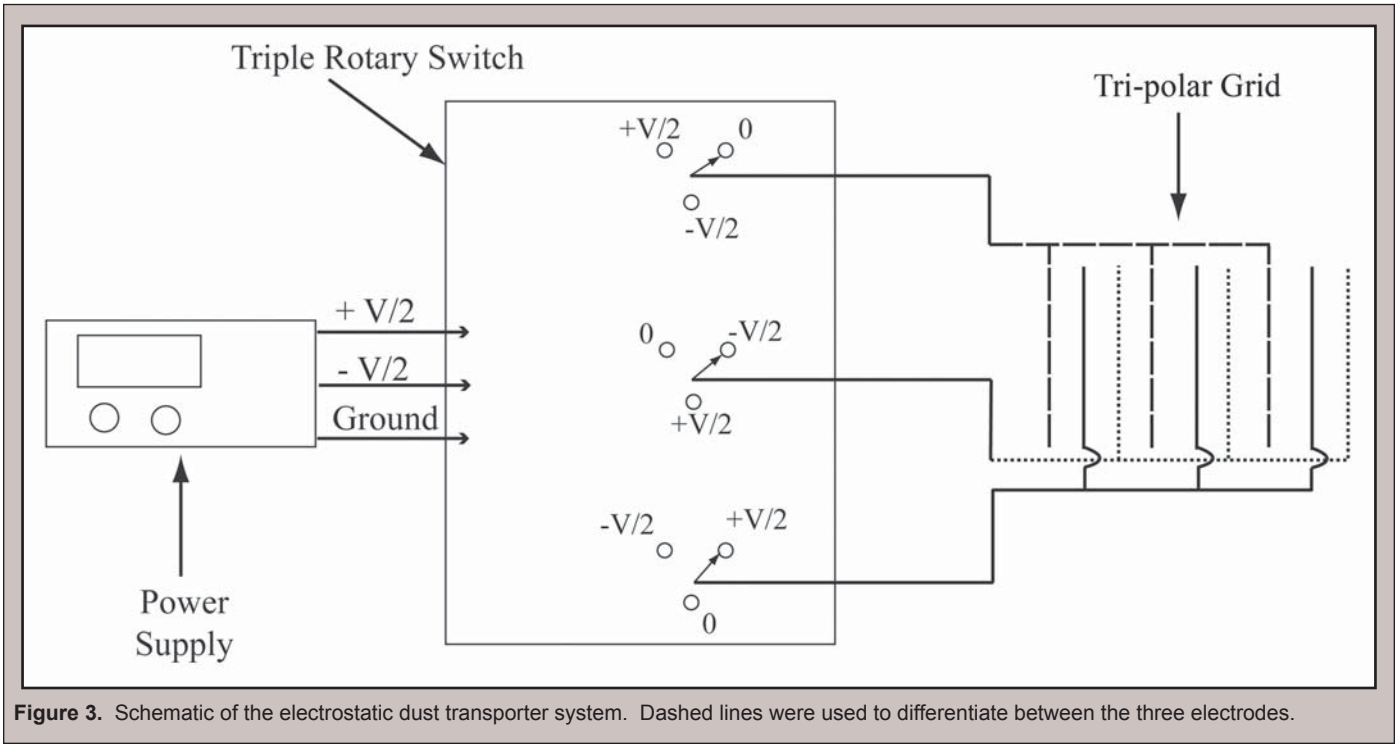

Figure 3. Schematic of the electrostatic dust transporter system. Dashed lines were used to differentiate between the three electrodes.

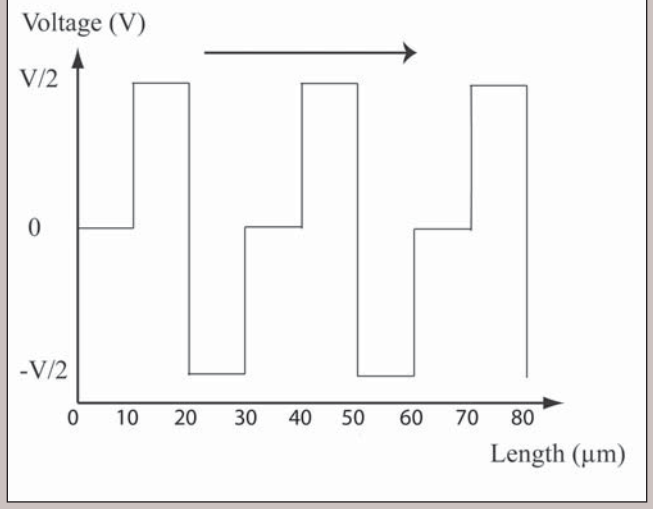

Figure 4. Schematic of the traveling electrostatic wave on the tri-polar grid with gold traces. The potential gradient is created by three different voltages on the three electrodes.

by the oscilloscope that corresponded to a number of half turns of the driver's control knob. A linear fit to the data was then obtained. The equation for this linear fit was used to predict the maximum voltage corresponding to 20 half turns of the control knob. The next short experiment consisted of measuring backing pressure as a function of the number of pulses provided to the piezoelectric valve. The initial backing pressure used was 40 psi, which was the maximum allowed by the initially available regulator. Equal pulses were continuously created to open the piezoelectric valve, and pressure was recorded after each pulse. We also measured pressure drop vs. backing pressure. Equal pulses were created at different backing pressures and the pressure drop was recorded after each pulse. Finally, we related pressure drop to voltage pulse width. First, a pulse with a specific length was created and the pressure drop was recorded. The backing pressure was then returned to its initial value of 100 psi, allowed by a new regulator. Finally, the process was repeated multiple times with varying pulse lengths.

After understanding the general characteristics of the gas puff system, tests were performed to find the most effective backing pressure, voltage pulse duration, and nozzle exit channel diameter and inclination. Tests were performed with sand placed on the surface of a 7.62 cm x 7.62 cm (3"x3") glass piece, at atmospheric pressure. To obtain the most effective backing pressure we first puffed helium to remove sand particles at different backing pressures. We then compared the resulting cleaned areas by observing pictures taken before and after puffing by a digital microscope. The backing pressures used were 40 psi, 60 psi, 80 psi and 100 psi. A schematic of the setup and nozzle location is shown in Figure 5. The same apparatus setup was used to obtain the optimal voltage pulse duration. We puffed helium to the surface of the glass containing sand particles using 250 ms, 500 ms, 750 ms and 1 000 ms pulse durations. We then compared the pictures taken with the digital microscope of the glass before and after the puff. To obtain the most effective nozzle exit channel diameter, we puffed gas on the sand particles with nozzles of different diameter. We compared the area cleaned by each nozzle by observing the pictures taken with the digital microscope. Finally, to obtain the most effective nozzle exit channel inclination, we used different nozzle orientations to puff on the sand particles and compared the pictures taken with the digital microscope.

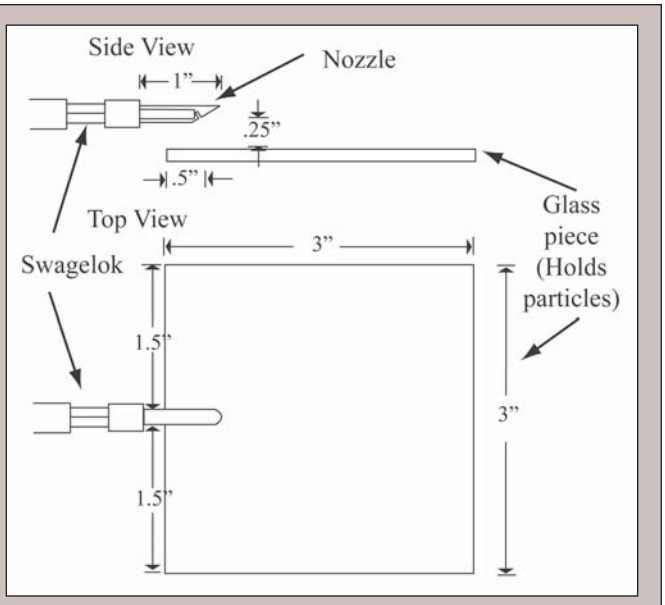

Figure 5. Schematic of setup used for tests to obtain the optimum backing pressure, voltage pulse width and nozzle exit channel diameter.

From the tests previously performed we obtained an optimal configuration that we used to puff sand particles, glass beads, carbon fiber composite (CFC) powder and tungsten particles at atmospheric pressure. Pictures were taken before and after the puff with both a digital microscope and a digital camera. Pictures taken with the camera provided a larger spatial coverage. After these tests were performed, puffing was done in a vacuum to simulate the dust environment. The nozzle and Swagelok were positioned inside a vacuum chamber, as shown in Figure 6. Sand, glass beads, CFC powder and tungsten particles were positioned on top of the 7.62 cm x 7.62 cm (3"x3") glass piece, which in turn was positioned on top of a tray inside the chamber. The base pressure for vacuum puffing was 1 mTorr. Pictures were again taken with a digital microscope and a digital camera, which showed the particles through a viewport on the upper side of the chamber. This setup is shown in Figure 6.

Electrostatic Dust Transporter System

Two types of tri-polar grid devices were tested. One consisted of chromium electrodes 25 μm thick and 25 μm apart; the other consisted of gold electrodes 10 μm thick and 10 μm apart. The electrodes are insulated with a 300 nm thick silicon nitride (SiN_x) layer. The grid devices were fabricated by the Princeton Macroelectronics Group using standard photolithography techniques. Carbon and tungsten particles were positioned on top of the tri-polar grid. Pictures of the particles on the grid were taken with a high resolution digital microscope before and after the electrodes were charged, and before and after every voltage switch caused by the triple rotary switch. The pictures obtained were later compared to observe any particle motion. Voltage switches with the triple rotary switch were manually performed every few seconds.

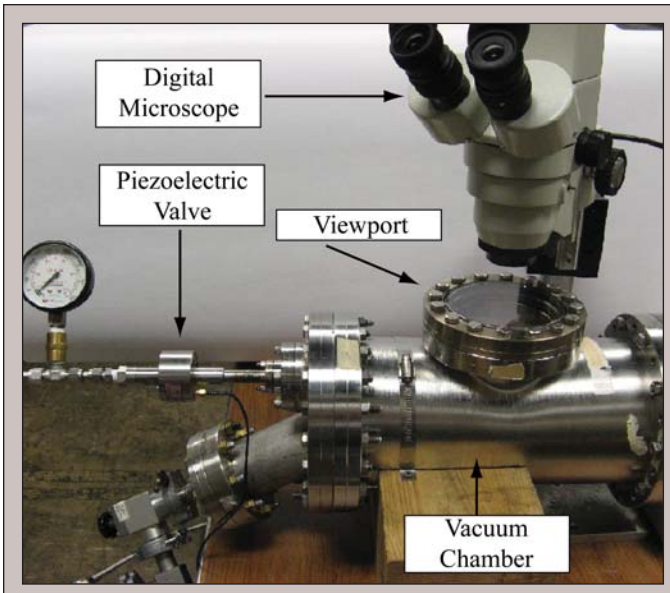

Figure 6. Setup used for vacuum puffing. The gas puff system is attached to the vacuum chamber's left side. The nozzle and Swagelok are inside the chamber.

Moreover, all tests were performed with grids that contained only two working electrodes, since fully functional grids were unavailable. Grids with two working electrodes produce a traveling electrostatic wave whose profile is different for each voltage switch. Nevertheless, potential gradients are still generated, which are responsible for particle motion.

Results

Gas Puff System

The first short experiments provided useful information regarding the properties and functioning of the system. The linear fit to the data points representing voltages given by the number of the control knob's half turns represented the data accurately. Thus, high confidence was placed on the accuracy of the predicted maximum voltage. This linear fit gave a maximum voltage of 170 V for 20 half turns of the control knob. The data points are shown in Figure 7. Also, backing pressure decreased as the number of pulses given increased, which showed correct functioning of our system and agreed with our expectations. Data for this experiment is shown in Figure 8. Additionally, the pressure drop is higher at high backing pressures, and lower at low backing pressures, as observed in Figure 9. This experiment indicated puffs with high backing pressures emit larger gas quantities and are expected to remove more dust particles. Finally, longer pulse widths gave bigger pressure drops and vice versa, as expected. The results are shown in Figure 10.

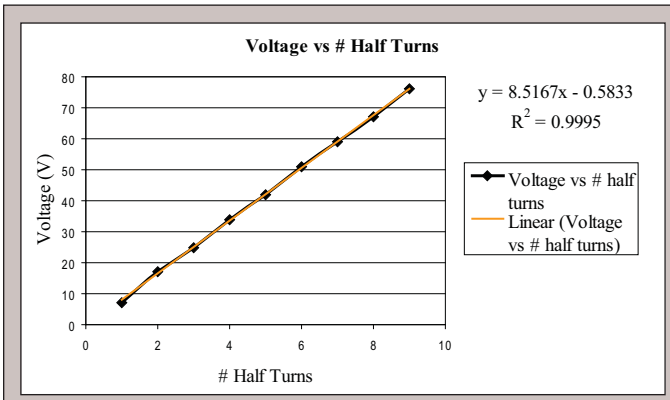

Figure 7. Driver output voltage vs. control knob. The oscilloscope had a maximum voltage range of 80 V. Higher voltage pulses produced by the driver were not observed with an oscilloscope, but were predicted with a linear fit shown on the upper right corner of the graph.

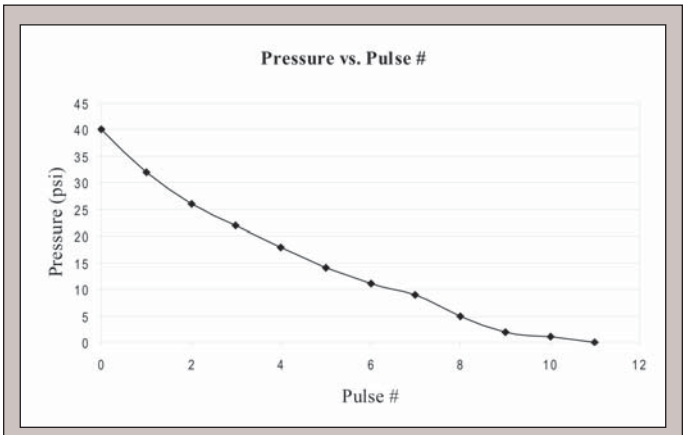

Figure 8. Backing pressure vs. number of pulses supplied. As expected, the pressure decreased as more pulses were provided. The pulse amplitude used for this test was 170 V.

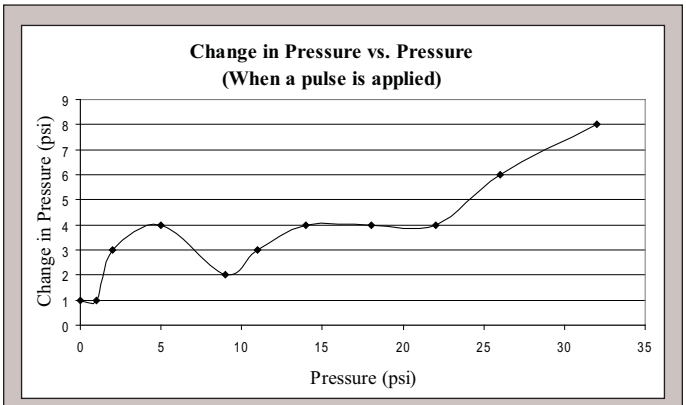

Figure 9. Change in pressure vs. backing pressure. For each pulse given, there is a big pressure drop when the backing pressure is high. Similarly, the pressure drop is small when the backing pressure is low.

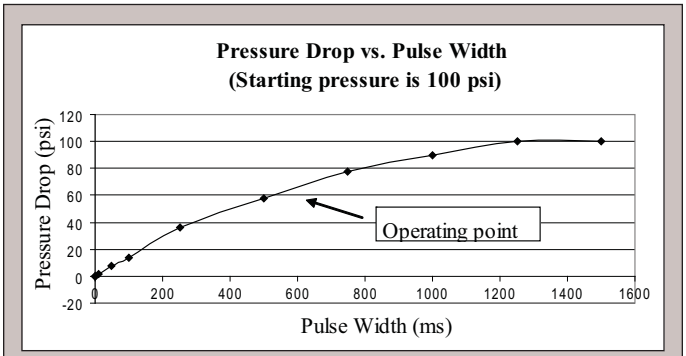

Figure 10. Pressure drop vs. pulse width. A large pulse width gives bigger backing pressure drops. All pressure drops were in reference to an initial backing pressure of 100 psi. The pulse width chosen for gas puffing was 500 ms.

Experiments performed to obtain the optimal configuration of the gas puff system yielded the following results. By observing pictures obtained with the microscope we concluded that higher backing pressures increased the area cleaned and that 100 psi was the most effective pressure allowed by our regulator. Moreover, longer pulse durations did not increase the cleaned areas, since most of the particles were removed within the first instances of the puff. Hence, to minimize the amount of gas wasted, a 500 ms pulse was chosen as the optimum, since it was as efficient as pulses with longer durations. Also, the nozzle with the smallest exit channel diameter, namely 0.34 mm, most effectively removed the particles. Finally, vertical puffing increased the area cleaned as opposed to horizontal puffing. However, space constraints limited puffing to an inclination of 45°. Thus, we decided to fabricate a nozzle with the maximum allowable exit channel inclination.

Both sand particles and glass beads were easily removed at atmospheric pressure with a puff, which created a 5 cm x 5 cm clean area. Carbon particles were also easily removed, giving a 4 cm x 4 cm clean area. Figure 11 shows pictures taken with the digital microscope and regular camera before and after puffing CFC powder at atmospheric pressures. Tungsten particles were harder to remove, since they adhered to the glass surface. The area cleaned for tungsten particles was around 3 cm x 3 cm at atmospheric pressure. Figure 12 shows pictures taken with the digital microscope and regular camera before and after puffing tungsten particles.

The cleaning effectiveness for vacuum puffing did not improve. Tungsten was again removed from a 3 cm x 3 cm area, carbon was cleaned from a 4 cm x 4 cm area, and sand and glass beads were removed from a 5 cm x 5 cm area. Figures 13, 14 and 15 show pictures of sand particles, CFC powder and tungsten particles in a vacuum, before and after the puff. Tungsten particles were dried by heating them in an oven for an hour, which minimizes moisture effects and makes them less adhesive to the glass piece. This process, however, did not improve the cleaning effectiveness.

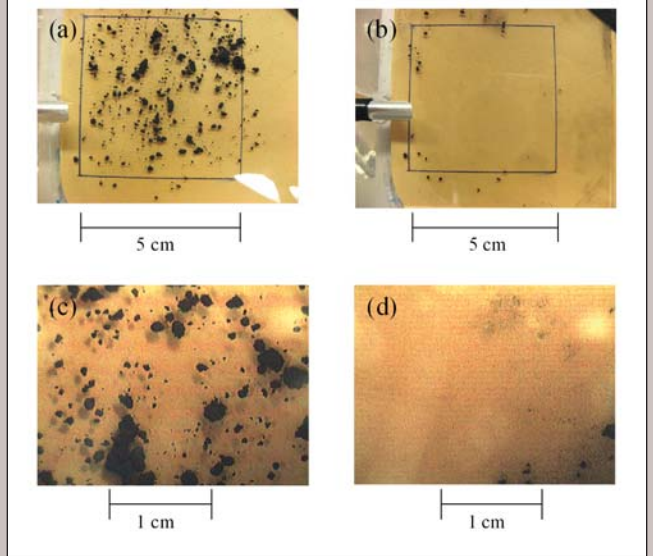

Figure 11. Pictures of carbon particles at atmospheric pressure taken (a) with digital camera before puff, (b) with digital camera after puff, (c) with digital microscope before puff and (d) with digital microscope after puff.

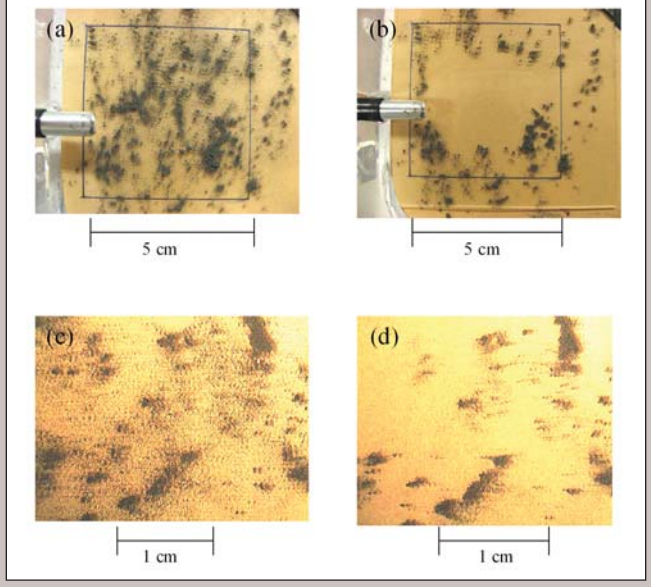

Figure 12. Pictures of tungsten particles at atmospheric pressure, taken (a) with digital camera before puff, (b) with digital camera after puff, (c) with digital microscope before puff and (d) with digital microscope after puff.

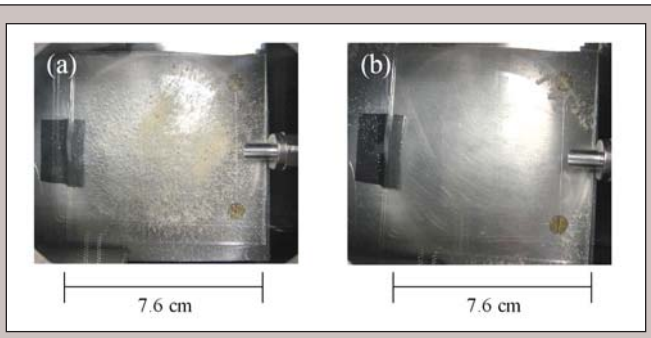

Figure 13. Pictures taken with digital camera of sand particles at base vacuum pressure of 1 mTorr (a) before and (b) after puffing.

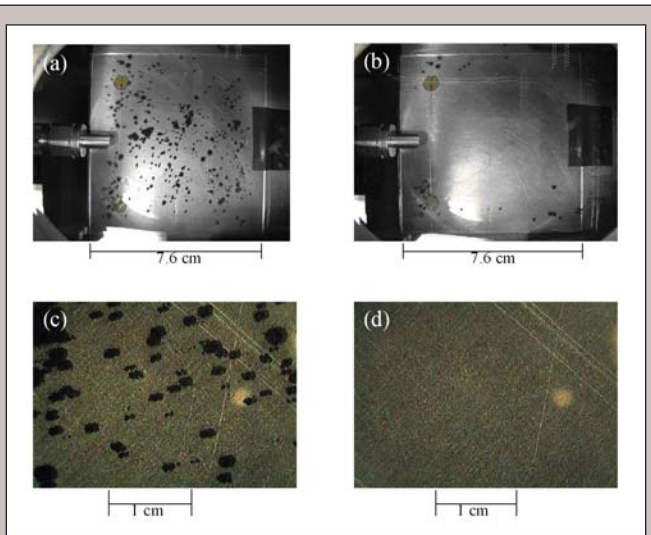

Figure 14. Pictures of carbon particles at base vacuum pressure of 1 mTorr taken (a) with digital camera before puff, (b) with digital camera after puff, (c) with digital microscope before puff and (d) with digital microscope after puff.

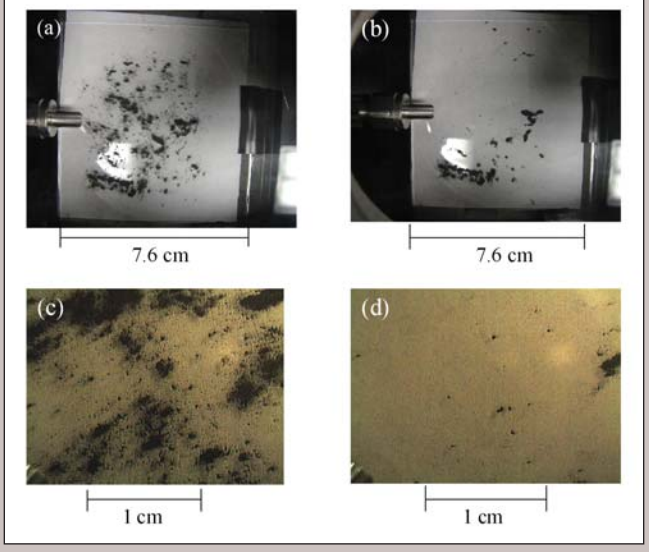

Figure 15. Pictures of tungsten particles at base vacuum pressure of 1 mTorr taken (a) with digital camera before puff, (b) with digital camera after puff, (c) with digital microscope before puff and (d) with digital microscope after puff.

Electrostatic Dust Transporter System

The results from the tests performed show particle motion. 50 V, 0.0 V and –50 V were applied to the triple rotary switch. When the power was turned on, motion of some particles was observed. As the voltages were sequentially switched more particle motion was observed. However, after one or two switches, particle motion stopped. Figure 16 shows two pictures, one of carbon particles on top of an uncharged tri-polar grid, and the other of carbon particles after the power was turned on. The red circles show a particle's location before the tri-polar grid was charged. After the voltages were supplied, the particles were not located within those circles, as shown by the second picture in Figure 16.

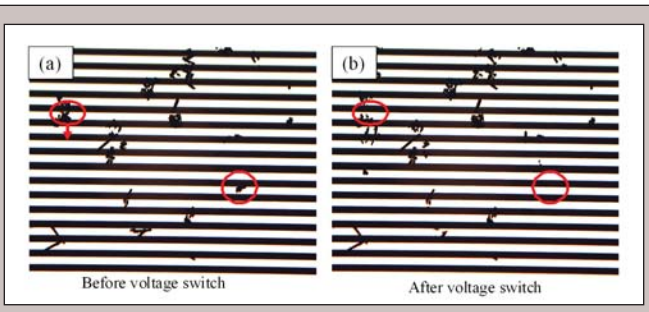

Figure 16. Images captured with a digital microscope of CFC powder on the surface of (a) an uncharged tri-polar grid and (b) a charged tri-polar grid. The red circles indicate some particles have been moved.

Discussion and Conclusion

Gas Puff System

The biggest electrostatic dust detector fabricated has a surface area of 5 cm x 5 cm. Our gas puff system was able to clear off carbon particles from a 4 cm x 4 cm area, which is very close to the required area. Tungsten particles were removed from a 3 cm x 3 cm area, which is a good achievement, yet it is not a large enough area to cover the entire surface of the detector. These results were achieved using the maximum allowed backing pressure. Therefore, tests should be performed to see if an increase of the exit flow momentum due to higher backing pressures increases cleaning effectiveness. Tests could be carried out with a gas puff system that has a regulator, pressure gauge and connecting tubes able to contain higher pressures. Additionally, tests should be conducted with a system containing two nozzles used to increase the emission of helium. This setup may be more effective at removing particles from the corners of the detector, where they are difficult to reach using our current system. Finally, simulations of the helium flow field on the surface of the glass piece could be performed with a computational fluid dynamics code, which may suggest better gas puff system designs.

Electrostatic Dust Transporter System

All research was conducted with grids that had only two functional electrodes. The tri-polar grids are very delicate since a light scratch easily damages an entire section or an electrode. More experience with their fabrication will make their manufacturing a faster process, and will also improve their quality and resistance. Despite using only two electrodes, the tri-polar grid produced some particle motion. This initial result suggests the electrostatic dust removal system is a feasible removal mechanism. As with the case of the gas puff system, further tests will be conducted in which a fully functional grid is used. Tests will be performed with this mechanism with the hope of obtaining unidirectional particle motion, which will better determine the ability of this system to transport dust particles.

Acknowledgments

This work was accomplished during a 2008 Summer Undergraduate Laboratory Internship supported by US DOE Grant No DE-AC02-76CH03073. I would like to thank my mentor, Charles Skinner, for his dedication and guidance. I would also like to thank Lane Roquemore, Jane Leisure and Sigud Wagner for additional advising. Finally, I would like to thank C. Bunting, M. Cropper, T. Holoman, R. Marsala and T. Provost for technical assistance and D. Boyle for previous work.

References

[1] C.H. Skinner, R. Hensley, A.L. Roquemore. "Large aperture electrostatic dust detector," in *Journal of Nuclear Materials*, Vol. 376, pp. 29–32, 2008.

[2] S. Ciattaglia, P.Andrew, A.Loarte, A.Martin, C.S. Pitcher, S.Rosanvallon, M.Shimada, W.Shu, C.H. Skinner, A.Tesini "An integrated approach of in-vacuum vessel dust and tritium inventory control in ITER" presented at 25th Symposium on Fusion Technology Conference, Rostock, Germany, 15–19 Sept. 2008.

[3] D.P. Boyle, C.H. Skinner, A.L. Roquemore. "Electrostatic dust detector with improved sensitivity," presented at 18th International Conference on Plasma Surface Interactions in Controlled Fusion Devices, Toledo, Spain, May 26–30, 2008.